Applied Catalysis B: Environmental 142–143 (2013) 259–267

Contents lists available at SciVerse ScienceDirect

Applied Catalysis B: Environmental

journal homepage: www.elsevier.com/locate/apcatb

Influence of pretreatments on commercial diamond nanoparticles on the photocatalytic activity of supported gold nanoparticles under natural Sunlight irradiation

David Sempere [a], Sergio Navalon [a,*], Mariana Dančíková [b], Mercedes Alvaro [a], Hermenegildo Garcia [a,*]

[a] Instituto Universitario de Tecnología Química CSIC-UPV and Departamento de Química, Universidad Politécnica de Valencia, Av. De los Naranjos s/n, 46022 Valencia, Spain
[b] Department of Organic Technology, Institute of Chemical Technology, Technická 5, 166 28, Prague, Czech Republic

ARTICLE INFO

Article history:
Received 3 April 2013
Received in revised form 29 April 2013
Accepted 8 May 2013
Available online 16 May 2013

Keywords:
Diamond nanoparticles
Thermal treatment
Gold supported
Sunlight assisted heterogeneous photo-Fenton reaction

ABSTRACT

Fenton-treated diamond (D) nanoparticles (NPs) are suitable support of gold to promote the wet peroxidation of phenol by H_2O_2. One of the drawbacks of this catalyst is the need of the pretreated commercial D NPs with a large excess of H_2O_2 and Fe(II) salts to remove the accompanying soot matter and introduce surface —OH groups on D. This process generates a large amount of waste waters and consumes large quantities of reagents, being desirable to develop alternative pretreatments for commercial D NPs. In the present manuscript we describe that a light combustion of the soot matter in a furnace under controlled temperature and time leads to a D support that after annealing at 500 °C under hydrogen affords a modified D material that is suitable as support of gold. We have found that annealing with hydrogen produces more efficient D samples than those without annealing or submitted to annealing under nitrogen. Characterization of the samples has shown that hydrogen annealing reduces surface C=O bonds to alcohols that are beneficial for anchoring gold nanoparticles. In this way, the resulting gold catalyst can set off the disappearance of phenol in water at pH 4 with only 2.6 equiv. of H_2O_2 assisted by Sunlight.

1. Introduction

Gold catalysis is attracting a continued interest due to the remarkable activity of gold to promote a large array of chemical transformations including aerobic oxidations [1], selective hydrogenations [2–4], epoxidations [2], homo- and cross-couplings [3,5], hydrosilylation [5] and many other types of reactions [5–8]. Since the seminal work of Haruta [9] showing the influence of particle size on the catalytic activity of supported gold materials, one of the main targets in the preparation of a supported gold catalyst is to reduce, as much as possible, the average particle size and to obtain samples with narrow size distribution. Although not completely understood, one of the roles of the solid supports is to stabilize gold nanoparticles (NPs) impeding their growth [5,10]. Accordingly, the target of the preparation procedure is to develop reliable protocols to form small Au NPs with narrow particle size distribution [10].

Recently, diamond (D) NPs have attracted attention as a convenient support for Au NPs [11–15]. In this context, we have recently reported that Fenton-treated D NPs are an extremely appropriate support for Au NPs with activity in the generation of hydroxyl radicals from H_2O_2 (Fenton reaction) [13]. Furthermore, while Fenton chemistry typically requires acid pH values [11,16–19], we have found that light-assisted Fenton degradation of phenol by Au/D can be carried out at quasi-neutral pH values [14,15]. Also, we have reported a study of the influence of the Fenton treatment conditions and preparation procedures on the catalytic activity of this material [12], the target being a decrease in the average Au particle size. Considering that D NPs are constituted by sp^3 carbon, it would be possible to modify the surface of this support in such a way that the resulting treated D samples are better suited as support leading during the deposition to smaller Au NPs. This variation in Au NPs particle size should be reflected in an increased catalytic activity.

While the Au/D samples obtained using Fenton-treated D NPs as support exhibit high activity as catalyst for the degradation of phenol by H_2O_2 [13,15], large scale implementation of this catalyst is limited by the fact that the Fenton oxidation consumes a large quantity of H_2O_2 and Fe(II) salts and generate a large volume of waste waters and iron sludges. It would be of interest to explore oxidative treatments of the D NP surface alternative to the Fenton

* Corresponding author. Tel.: +34 620 952 690; fax: +34 96387 7809.
E-mail addresses: dasemar1@etsii.upv.es (D. Sempere), sernaol@doctor.upv.es (S. Navalon), mariana.dancikova@gmail.com (M. Dančíková), malvaro@qim.upv.es (M. Alvaro), hgarcia@qim.upv.es (H. Garcia).

0926-3373/$ – see front matter © 2013 Elsevier B.V. All rights reserved.
http://dx.doi.org/10.1016/j.apcatb.2013.05.016

oxidation that could render the preparation of Au/D environmentally friendlier. The target is to carry out a thermal treatment under controlled aerobic atmosphere inducing a light surface oxidation of the D NPs that can be considered as an equivalent treatment to the chemical Fenton oxidation. In the present manuscript we report that an aerobic thermal treatment followed by a subsequent hydrogen annealing leads to Au/D samples with suitable catalytic activity for the light-assisted degradation of phenol consuming low H_2O_2 excess and avoiding the need of Fenton pre-treatment of D NPs. This represents a significant advance in catalyst preparation from the environmental point of view. The interest of our work is to show that surface modification of D NPs can be carried out by shallow oxidation of the surface.

2. Experimental

2.1. Materials

H_2O_2 solution in water (30%, v/v), phenol (≥99%), HNO_3 (65%), HCl (37%, ACS reagent), H_2SO_4 (98%), $HAuCl_4{\cdot}3H_2O$, NaOH (ACS reagent) and diamond nanopowder (ref: 636444, 95%) were commercial samples from Sigma–Aldrich. Milli-Q water was used in all the experiments. The other reagents used were of analytical or HPLC grade.

2.2. Diamond functionalization and catalyst preparation

Thermal treatments of commercial D NPs were carried in a furnace at 420 °C exposed to the ambient atmosphere. Briefly, 0.5 g of raw diamond nanopowder was heated in an oven under static air (not dried) at 7 °C min^{-1} up to 420 °C and then maintained for 5 h. This sample was denoted as F (meaning furnace). Additionally, the F sample was submitted to a subsequent annealing treatment under continuous N_2 or H_2 flow. In particular, the F sample was placed in a quartz reactor under either N_2 or H_2 flow (100 mL min^{-1}) and heated using a ramp of 8 °C min^{-1} up to 500 °C and maintained for 6 h. Then, the sample was cooled at room temperature and labelled as FN_2 or FH_2, respectively.

Preparation of Au/F, Au/FN_2 and Au/FH_2 catalysts was accomplished using the polyol method [20,21]. Briefly, 200 mg of the diamond support (F, FN_2 or FH_2) were suspended in 80 mL of ethylene glycol and sonicated for 30 min. Then, the corresponding amount of gold salt dissolved in water was added to the diamond suspension to achieve the required gold loading (from 0.1 to 0.5 wt.%). The suspension was heated up to 85 °C under vigorous stirring and allowed to react for 4 h. After cooling the reaction at room temperature, the suspended powder was recovered by centrifugation at 14,000 rpm. Then, the supernatant was removed and the catalyst dispersed in ethanol and washed by performing three consecutive centrifugation-re-dispersion cycles with ethanol, acetone and three more using water. Finally, the catalysts (Au/F, Au/FN_2 and Au/FH_2) were freeze-dried.

2.3. Characterization

Quantitative Fourier transformed infrared (FT-IR) spectra of the different samples were recorded on a Nicolet 710 FTIR spectrophotometer by using KBr disks of the samples prepared pressing the wafers (10 mg) at 10 T for 2 min. Elemental analyses were determined for samples equilibrated to the ambient using a Perkin Elmer CHNOS analyzer. Solid-state ^{13}C NMR spectroscopy was recorded in a Bruker AV 400 instrument. Temperature-programmed desorption (TPD) coupled to a mass-spectrometer (TPD-MS) was carried out in a Micrometer II 2920 connected to a mass-spectrometer. In particular, TPD was carried out using 100 mg of sample under helium, heating from room temperature to 900 °C at 10 °C min^{-1}. X-ray photoelectron spectroscopy (XPS) measurements were performed on a SPECS spectrometer with a MCD-9 detector using a monochromatic Al (K_{alpha} = 1486.6 eV) X-ray source. Spectra deconvolution has been performed using the CASA software and binding energies were referenced to the C 1s peak at 284.4 eV [22]. Zeta potential measurements were carried out using a Zetasizer ZS nano (Malvern instruments). In particular, the zeta potential of aqueous suspension of D materials (10 mg L^{-1}) was determined adjusting at the required pH value using HCl (0.1 M) or NaOH (0.1 M). The specific Brunauer–Emmett–Teller (BET) surface area was measured using a ASAP 2010 Micrometrics device.

Metal loading (0.5, 0.2 and 0.1 wt.%) on the D NPs was determined by inductively coupled plasma atomic emission spectroscopy (ICP-AES). The percentage of gold leached from the solid catalyst to the solution was determined by ICP-AES analyses of the filtered samples (0.2 μm Nylon filters) at the end of the reaction. The detection limit of the technique was 0.1 mg L^{-1}. X-ray diffractograms (XRD) were recorded by using a Philips X-Pert diffractometer equipped with a graphite monochromator, operating at 40 kV and 45 mA and employing Ni filtered CuKα radiation (λ = 0.1542 nm). Transmission electron microscopy (TEM) and high resolution TEM (HRTEM) of the different samples were obtained using a TECNAI G2 F20 (FEI) instrument operating at 200 kV with a resolution of 0.24 nm. The particle size distribution was estimated by counting over 300 particles.

2.4. Photocatalytic experiments

Catalytic experiments were carried out under natural Sunlight irradiation and measuring the phenol disappearance and H_2O_2 decomposition. Briefly, 100 mL of aqueous phenol solution (100 mg L^{-1}) was placed in a 500 mL round bottom flask. Then, the desired amount of the catalyst was added and the system sonicated for 10 min. Once the pH was adjusted using aqueous solutions of HNO_3 (0.1 M) or NaOH (0.1 M), the samples were exposed to the Sun and the required amount of H_2O_2 was added to start the reaction. It should be commented that during the reaction the pH value decreases due to the degradation of phenol and the formation of carboxylic acids [11]. To minimize gold leaching from the heterogeneous catalyst to the solution the pH value was not allowed to be lower than 4.

Time conversion of phenol was determined by analyzing aliquots (2 mL, filtered through 0.2 μm Nylon filter) by reverse-phase Kromasil-C18 column using H_2O/CH_3OH/acetic acid, 69:30:1, as eluent under isocratic conditions and employing an UV detector. The residual H_2O_2 was determined by 10-fold dilution of the reaction mixture and using $K_2(TiO)(C_2O_4)_2$ (Aldrich) in H_2SO_4/HNO_3 as colorimetric titrator. The solution was allowed to react for 10 min before monitoring the intensity at 420 nm.

Reuse experiments were performed recovering the catalyst at the end of the previous cycle by filtration through a 0.2 μm Nylon membrane. The catalyst was washed with Milli-Q water at pH 10 and then rinsed with Milli-Q water in order to remove excess of base and salts. It should be commented that washings with basic water were carried out in order to remove possible carboxylic acids formed as degradation products that could deactivate the gold catalyst [11,23]. The recovered catalyst was used for the next run with appropriate substrate and solvent. When studying the reusability, the samples are submitted to natural Sunlight solar irradiation that can vary on a daily basis. Therefore, a control sample was simultaneously run using a fresh catalyst, which provides a better comparison than a run of the same fresh catalyst on a different day.

Table 1
Gold supported on functionalized commercial D.

Entry	Sample	Support preparation	Gold loading (%)[a]
1	Au/F	D calcination at 420 °C for 6 h giving rise to F support	0.5
2	Au/FN_2	F support and subsequent thermally annealed at 500 °C under N_2 for 6 h giving rise to FN_2 support	0.5
3	Au/FH_2	F support and subsequently submitted to thermal treatment at 500 °C under H_2 for 6 h giving rise to FH_2 support	0.5
4	Au/FH_2	FH_2 support	0.2
5	Au/FH_2	FH_2 support	0.1

[a] Based on chemical analysis of the solution after gold deposition

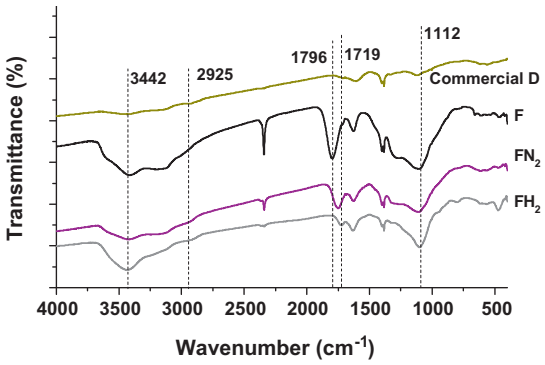

Fig. 1. FT-IR of commercial and D-functionalized samples.

Quenching experiments using dimethyl sulfoxide (DMSO) as selective hydroxyl radical (•OH) were carried out by adding to the reaction a DMSO-to-H_2O_2 molar ratio of 10 [14].

Sunlight intensity was measured using a photodiode connected to a voltmeter. On average, the solar irradiation was $0.8 \pm 0.18\ mW\ cm^{-2}$ during the experiments performed in this study. Ambient and solution temperatures were, on average, 30.6 ± 2.6 and 26.9 ± 1.8 °C, respectively.

3. Results and discussion

3.1. D characterization

Our work starts with commercial D NPs (<10 nm) that are embedded in a soot matter of amorphous carbon [13,24]. Purification of commercial samples was carried out by controlled thermal oxidation under aerobic conditions at moderate temperature (420 °C). This temperature was selected based on previous reports that have shown that the soot matter of commercial D can be selectively combusted without producing the complete combustion of diamond at this temperature [24].

After controlled combustion of the soot matter, the D sample, labeled as F, was submitted to a H_2 or N_2 annealing at 500 °C. Then, gold was loaded in the different supports using the polyol method. Table 1 lists the Au/D samples studied in the present work including the preparation conditions and other relevant characterization properties.

The purpose of this thermal annealing under H_2 was to cause {AQ:} the reduction of presumed carboxylic groups as well as the decomposition of esters and anhydrides leading to a surface in which ideally only hydroxyl groups or CH groups should be present. While annealing in the presence of H_2 can produce the reduction of carbonyl and carboxyl groups to alcohols, analogous treatment under N_2 should only lead to partial thermal decarboxylation and decomposition of anhydrides, ethers and lactones without hydrogenation of the surface. Therefore, depending on the H_2 or N_2 atmosphere during the thermal annealing after oxidation differences in the density of hydroxyl groups are expected. Since we have observed that the presence of hydroxyl groups on D nanoparticles plays a role stabilizing Au NPs [13], differences in the catalytic activity between the samples prepared with N_2 or H_2 annealing arising from the particle size distribution and Au NP-support interaction could be possible.

The samples (commercial D, F, FH_2 and FN_2) were characterized by FT-IR, elemental analysis, BET surface area, XPS, TPD-MS and also by the zeta potential of colloidal solutions. Fig. 1 shows a set of FT-IR spectra corresponding to the D samples. FT-IR spectroscopy of F shows a broad band from 3650 to 2700 cm^{-1} and vibrational structure that can be attributed to the stretching of —OH groups in carboxylic acids. In the C=O region, an intense peak at 1796 cm^{-1}, probably corresponding to anhydrides is accompanied by a shoulder at 1719 cm^{-1}, compatible with the presence of carboxylic groups. The thermal treatment with H_2 produces a change in the —OH vibration zone with a more symmetric —OH band appearing at 3442 cm^{-1} characteristic of alcohols and even —CH vibrations at 2925 cm^{-1} resulting from hydrogenation of carbons. These changes in the —OH region were accompanied by a complete disappearance of the intense anhydride band and a decrease intensity of the C=O at 1719 cm^{-1} for the FH_2 sample. When the annealing treatment was carried out under N_2, a decrease in the intensity of the —OH bands from 3650 to 2800 cm^{-1} was also observed but the shape of the —OH band was similar, and lower intensity, to that of the F precursor. It is important to note that a significant decrease of the intensity of the C=O band is also observed in the FN_2 sample, the maximum of the C=O peak appearing now at 1760 cm^{-1} that matches with the expected wavenumber of lactons [25]. When comparing the annealing under N_2 or H_2, as it was anticipated considering the possibility of chemical reduction, the H_2 treated sample exhibited higher intensity of —OH vibration band and a developed peak of alcohol —OH groups. In addition, the sample annealed with H_2 has also lower intensity in the C=O vibration region compared to annealing under N_2. All together these FT-IR spectroscopic data indicate that besides the thermal decomposition of carboxylic acids and formation of esters taking place under N_2, the presence of H_2 influences an additional reduction of C=O bonds leading to an increase in the population of —OH.

The previous FT-IR spectroscopic study is compatible with the variations in the chemical analysis of the solids (Table 2). In all cases a reduction of oxygen content is observed during the annealing regardless if the process is carried out under N_2 or H_2. However, when the annealing is carried out under H_2 the increase in the relative proportion of H/C with respect to the case of N_2 treatment indicates that the treatment has led to the addition of hydrogen into the solid. In addition, the thermal treatments slightly increase the BET surface area with respect to the commercial D sample.

The samples were also characterized by solid-state ^{13}C NMR spectroscopy. Fig. 2 shows the block decay (BD) and ^{1}H ^{13}C-cross polarization ^{13}C NMR spectra recorded for the samples to illustrate the changes observed. According to the low relaxation of rigid quaternary carbons, BD spectra of the samples only allow to detect

Table 2
Elemental analysis[a] and S_{BET} of commercial and D-functionalized samples.

	N (%)	C (%)	H (%)	O (%)	H/C molar ratio	S_{BET} ($m^2\ g^{-1}$)
Commercial D	2.5	89.1	1.0	7.5	0.13	273
F	2.5	84.8	0.3	12.3	0.04	320
FN_2	2.6	88.1	0.5	8.9	0.07	327
FH_2	2.6	89.2	0.8	7.4	0.11	328

[a] For ambient equilibrated samples.

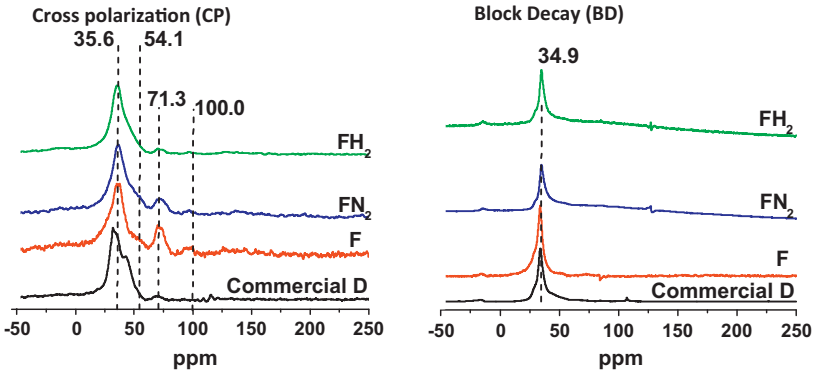

Fig. 2. ^{13}C-NMR spectra of commercial and D-functionalized D samples.

the core carbons centered at 33.6 ppm that correspond to majority of the C atoms present in the samples, but did not reveal differences depending on the calcination or annealing treatments. In contrast, cross-polarization technique with magnetization transfer from ^{1}H to ^{13}C becomes very informative with respect to the functional groups introduced under the different treatments, making possible to correlate these changes with FT-IR spectroscopy. In particular, two bands are appearing at 71.3 and 54.1 ppm, the later as a shoulder of the signal corresponding to the core carbons, show the structural changes taking place in the samples (F, FH_2 and FN_2) depending on the treatment. In particular, the 71.3 ppm peak not present in the commercial D sample appears in the F sample, after mild calcination at 420 °C under air, and is attributable to the generation of ester groups since they would correspond to the alcoxy carbons of the ester functionality. This signal is highly intense after the oxidation of the commercial D sample at 420 °C. Subsequent annealing under N_2 reduces the intensity of this peak, in agreement with partial lose of ester groups observed in FT-IR. When the annealing is carried out under H_2, the 71.3 ppm peak almost completely disappears indicating that this pretreatment is the most appropriate to remove this type of surface functional groups. Similar trend, although less clear due to the overlap with the 35.6 ppm core carbon peak was also observed for the 54.1 ppm signal. Thus, this shoulder appears during the process of calcination under aerobic conditions and then subsequently reduces intensity during the annealing, particularly under H_2. We attribute this 54.1 ppm shoulder to surface carbons bonded to oxygen in alcohol groups that become partially converted into C=O (treatment under N_2 or H_2) or even to C—H moieties (in the case of the treatment under H_2).

In order to provide additional information we proceeded to obtain the TPD-MS profile of the set of four samples. TPD is a technique that has been widely applied to characterization of carbons and there is considerable information in the literature for a safe assignment of the TPD peaks [25,26]. Thus, it is known from the literature that groups like carboxylic acid, lactones and anhydrides present in the carbon sample decompose losing CO_2. Other oxygenated functional groups such as carbonyl units and ether linkages decompose at higher temperatures by expelling CO. Therefore, evolution of CO_2 occurring at lower desorption

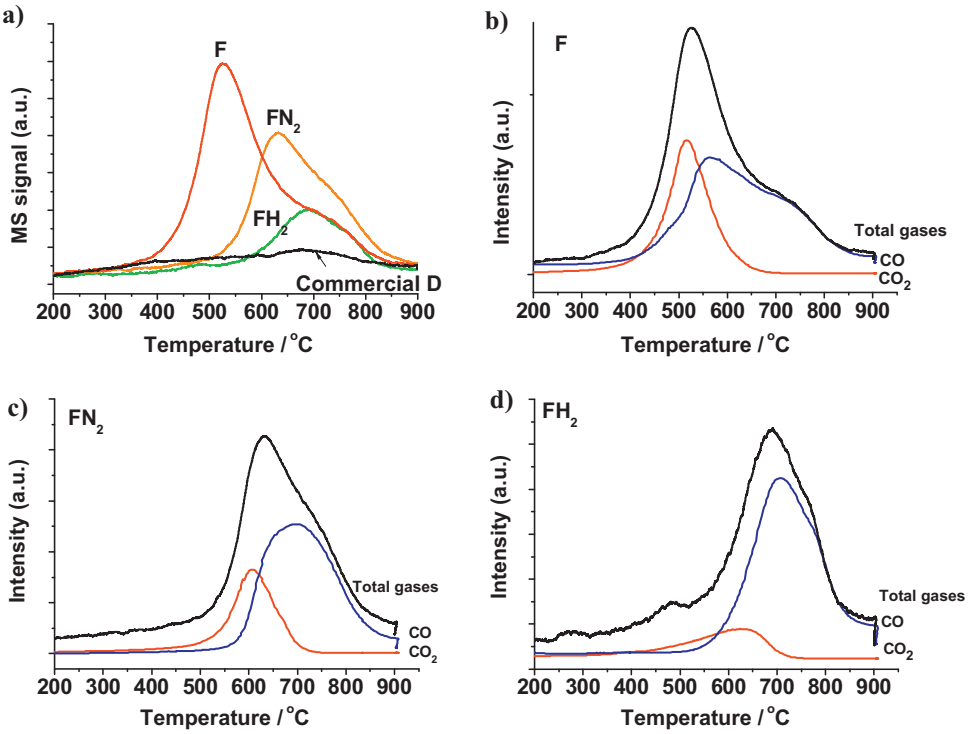

Fig. 3. TPD (a) and TPD-MS (b, c, d) of commercial and D-functionalized samples.

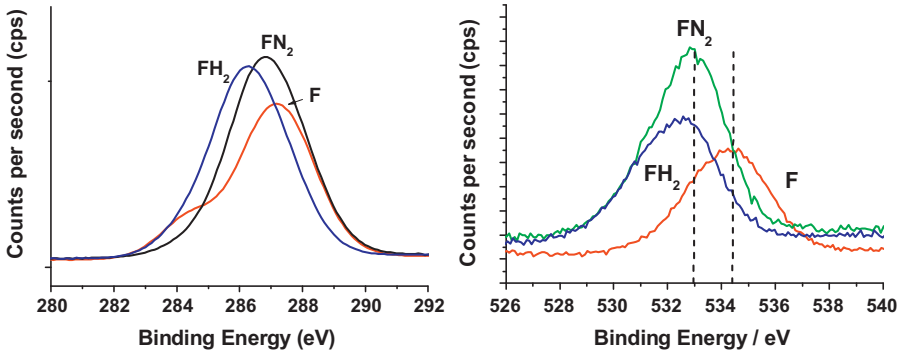

Fig. 4. XP spectra of C 1s (left) and O 1s (right) of the D-functionalized samples.

temperatures is indicative of carboxylic groups and its derivatives [25,26]. The TPD-MS data for the four D samples are presented in Fig. 3 (see also Fig. S1 for TPD-MS of commercial D NPs).

A comparison of the experimental profiles nicely indicate that annealing remarkable reduces the absolute intensity of the total gases evolved (Fig. 3a). The residual CO_2 and CO profiles after annealing (Fig. 3c and d) appearing at higher temperatures compared to F sample (Fig. 3b). These two effects on the CO_2 and CO profiles are more marked when the annealing is carried out under H_2. All together, TPD-MS profiles can be interpreted considering that annealing leads to decarboxylation (characterized by a loss of CO_2 at low temperatures), loss of lactones and anhydrides (characterized by loss of CO_2 or $CO_2 + CO$, respectively), being the CO profiles observed after annealing attributable to residual carbonyl and ether groups [26].

XPS is also a very informative technique to characterize carbon materials and there is considerable literature information about thems [26–28]. In fact, the C 1s peak is standard and reference in this type of spectroscopy. Fig. 4 shows the C 1s and O 1s XP spectra of the different D supports. Annealing under H_2 produces in both cases a shifting of the signals to lower binding energy values indicating the reduction of sp^2 carbon and oxygen functional groups.

In addition, Fig. 5 shows selected XP spectra to illustrate the deconvolution of the peaks and the changes occurring during the treatment with H_2. Thus, the C 1s peak of the three samples could be adequately deconvoluted to three components corresponding to core carbons (carbon atoms tetracoordinated to four C atoms), C bonded to —OH or ethers and C=O (Fig. 5a, b and Fig. S2). In agreement with the previous characterization by FT-IR and TPD-MS, the parent F sample has these three main components, the major one being attributable to C=O (Fig. 5a and b). The annealing treatment either under N_2 (Fig. 2S) or H_2 (Fig. 5c and d) shifts the maximum of the binding energy to lower values and change the distribution among the three peaks, the major component was the C bonded to —OH or ether. These changes are compatible with the thermal decarboxylation of carboxylic acids, esters, lactones and anhydrides as observed in FT-IR and TPD-MS. Similarly, the changes in the O 1s XPS peaks also reflect the disappearance of sp^2 oxygens leading to

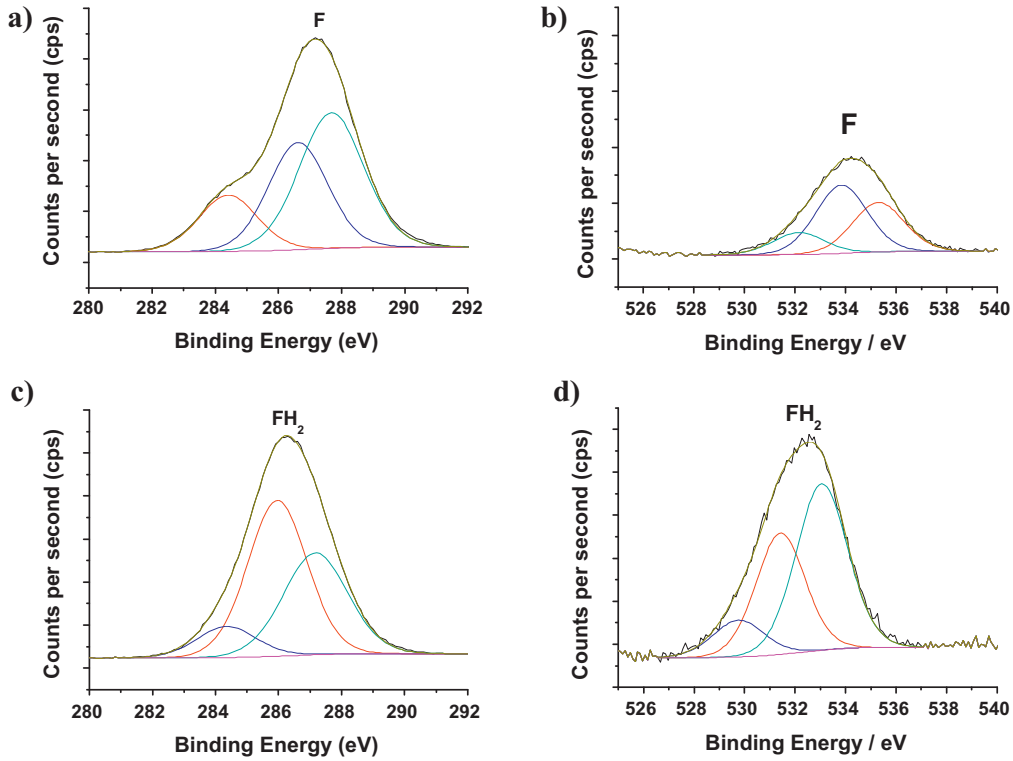

Fig. 5. Deconvoluted C 1s (panels a and c) and O 1s (panels b and d) XP spectra of F (a and b) and FH_2 (c and d) samples.

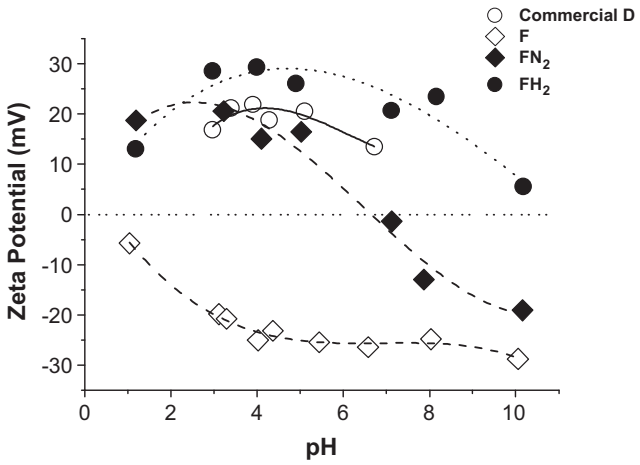

Fig. 6. Zeta potential of commercial and D-modified samples as a function of the pH.

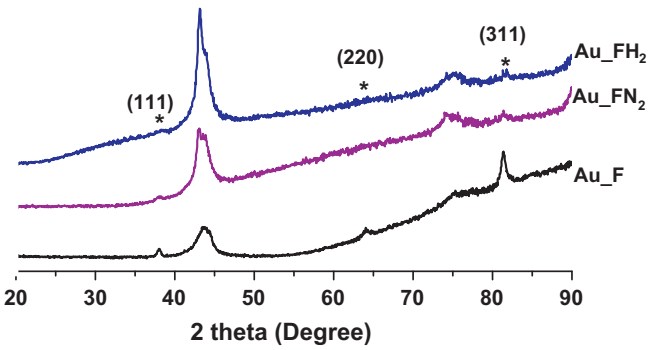

Fig. 7. Powder XRD of Au NPs supported D-samples. The peaks labeled with asterisks correspond to characteristic Au diffraction peaks for the facets indicated in the plot.

a shift to lower binding energies after annealing treatment (Fig. 5b, c and Fig. S2).

Furthermore, we recorded the zeta potential of aqueous D suspensions at different pH values as shown in Fig. 6. These measurements also allow characterizing the functional groups of the different samples. For example, carboxylic acids have commonly pK_a values between 4 and 5. Thus, at pH values higher than 5 the zeta potential will be negative while values lower than 4 will rise positive zeta potential values. In our case, the pattern corresponding to the F sample presents a wide range of negative Z

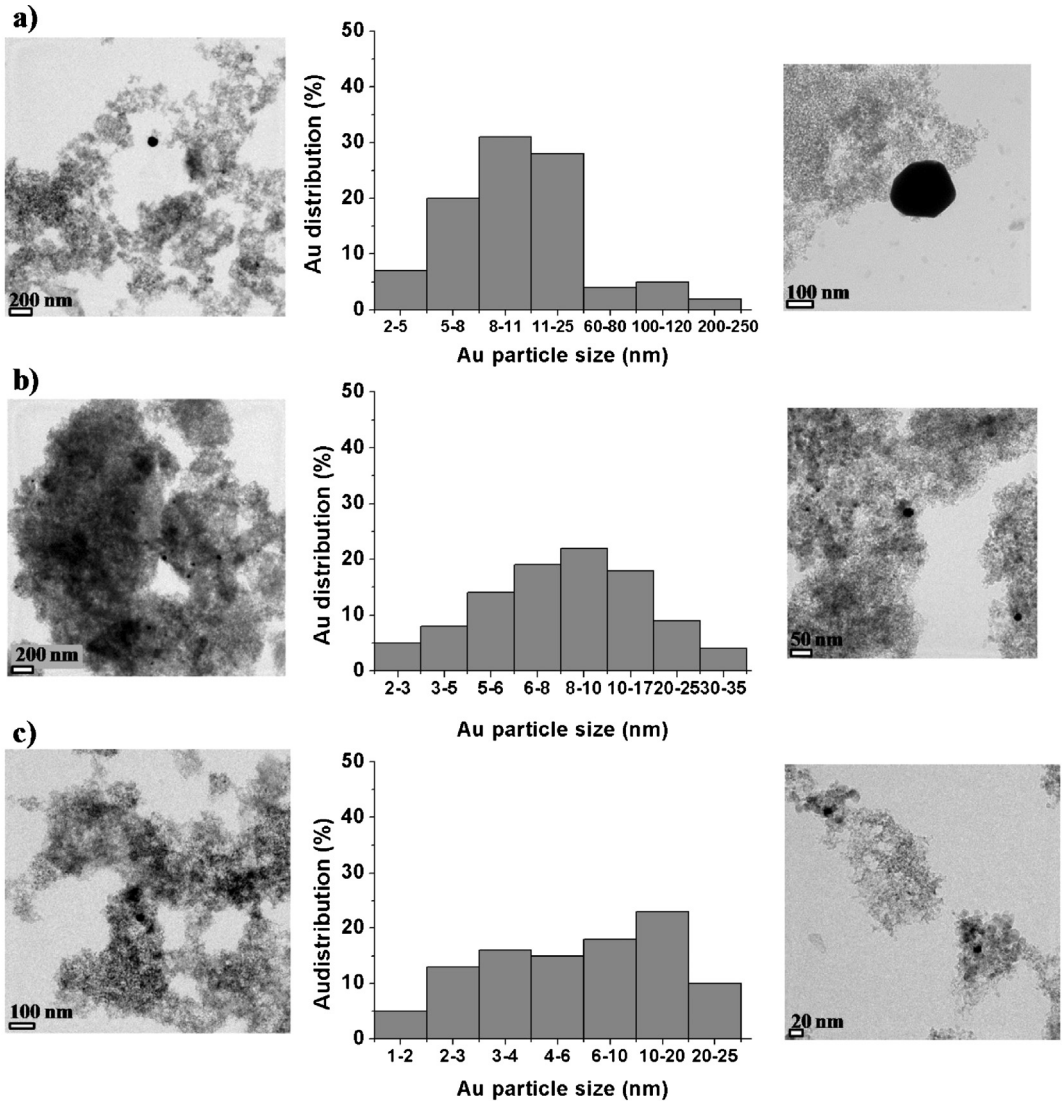

Fig. 8. TEM images and particle size distributions of (a) Au(0.5%)/F, (b) Au(0.5%)/FN_2 and (c) Au(0.5%)/FH_2.

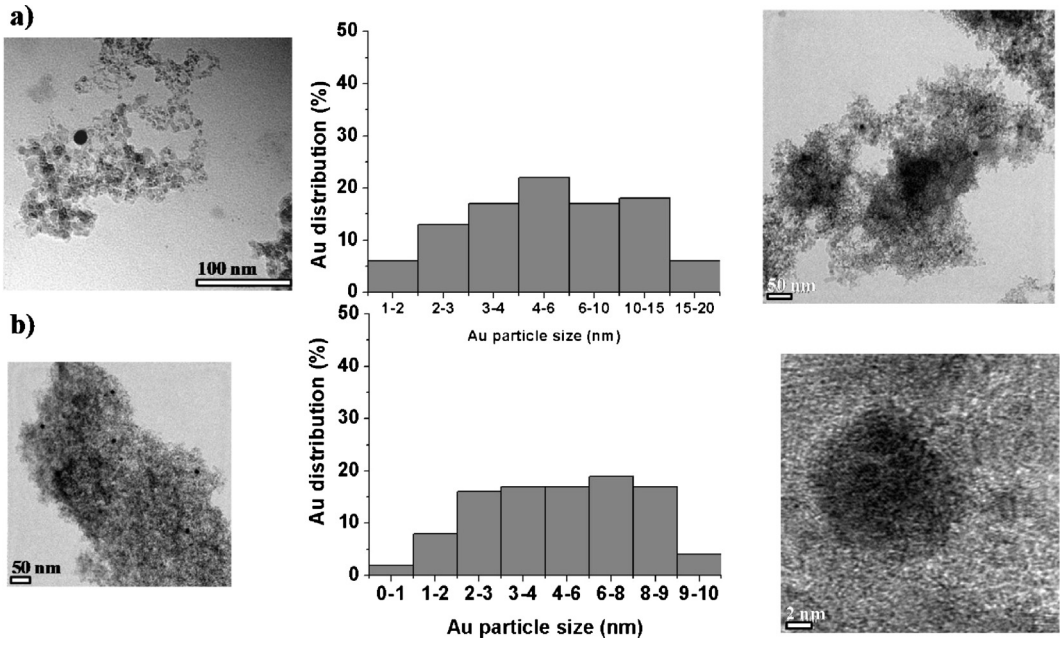

Fig. 9. TEM images and particle size distribution of (a) Au(0.2%)/FH_2 and (b) Au(0.1%)/FH_2.

potential as a function of the pH indicating the presence of acid functionalities. As expected, annealing of the F sample under N_2 or H_2 produces a reduction of these acids groups. In particular, the positive zeta potential for the FH_2 sample agrees with the previous data indicating the absence of carboxylic groups but the presence of hydroxyl groups.

3.2. Au NPs deposition

With the functionalized D samples (F, FN_2 and FH_2) we proceeded to deposit Au NPs following the procedure known as the polyol method. This method consists in heating in ethylene glycol a solution of $HAuCl_4$ in the presence of the support. During this process ethylene glycol reduces Au(III) to Au NPs that become deposited on the surface of the D solids [29]. The advantage of this well-established protocol with respect to other alternative procedures such as deposition-precipitation method is a complete deposition of all the gold present in the system onto the solid as well as reproducibility in the particle size distribution and shorter preparation times [29].

The analytical data of the Au/D samples prepared are contained in Table 1. The samples were prepared on purpose to have a gold loading of 0.5 wt.%, or below, since it has been shown that higher loadings are detrimental with respect to their catalytic activity [5]. The resulting samples were characterized by powder XRD (Fig. 7). It was observed that in addition to the peaks corresponding to the diamond support [12] appearing at 43 and 75°, peaks corresponding to the (1 1 1), (2 2 0) and (3 1 1) facets of gold at 37, 64 and 78°, respectively, were also observed in some of the samples (Fig. 7) [12,30]. Interestingly, it was observed that the intensity and width of the peaks follow a clear trend depending on the pretreatment, Au/F exhibiting the highest peak intensity that decreases when the annealing is carried out under N_2 and undergoes further decrease when the annealing is under H_2. We interpret this observation of XRD peaks of Au NPs as indicating a decrease in the average particle size depending on the annealing treatment. The samples with largest particles being those that exhibit more intense XRD peaks.

The conclusions based on XRD were confirmed by TEM, where Au NPs can be clearly observed. Figs. 8 and 9 show selected TEM images representative of the corresponding series of Au/D samples. The same figure also contains a statistical analysis of particle size distribution for each of the samples under study. The important issue was that the average particle size and the particle size distribution are strongly influenced by the thermal treatments of the D (Fig. 8) and the gold loading (Fig. 9). Additional TEM and HRTEM images are collected in Fig. S3. In agreement with our assumption, adequate surface modification is necessary in order to achieve an optimal deposition of gold and, as we will show latter, catalysts with improved catalytic activity.

In this way, after mild oxidation by thermal treatment, the resulting Au/F sample exhibits a broad particle size distribution centered at 22.5 nm with the presence of very large gold particles up to 250 nm. Annealing under N_2 leads to a decrease in the average particle size to 10.2 nm and a reduction of the dispersion of their size. The lowest average particle size is achieved when the F support was annealed under H_2 that results in a average diameter of the Au NPs of 8.7 nm, very large Au NPs being not observed at all in this sample. For Au/FH_2 samples with gold loadings of 0.2 and 0.1 wt.% the average particle size was 6.8 and 5.1 nm, respectively, and the size distribution narrower (Fig. 9).

3.3. Photocatalytic activity

As commented in the introduction the aim of the present work is to determine if alternative surface oxidation treatments can produce D supports suitable for their use as heterogeneous gold catalysts without the need of using Fenton treatments that require large amounts of reagents and generate considerable wastes. Aimed at this goal, the next step after preparation and characterization of Au/D samples was evaluation of their catalytic activity for the natural Sunlight assisted degradation of phenol as a probe by H_2O_2. The figure of merit of this reaction is disappearance of phenol over the reaction time and H_2O_2 consumption. In principle, according to what is known in gold catalysis in general and for this reaction in particular, it can be anticipated that Au samples with lower Au particle size should exhibit higher catalytic activity [10,12]. As it can be seen in Fig. 10, this well-known relationship between particle size and catalytic activity [9,12] is also observed in the present case, the most active sample being those in which this support was first oxidized thermally and subsequently annealed under H_2.

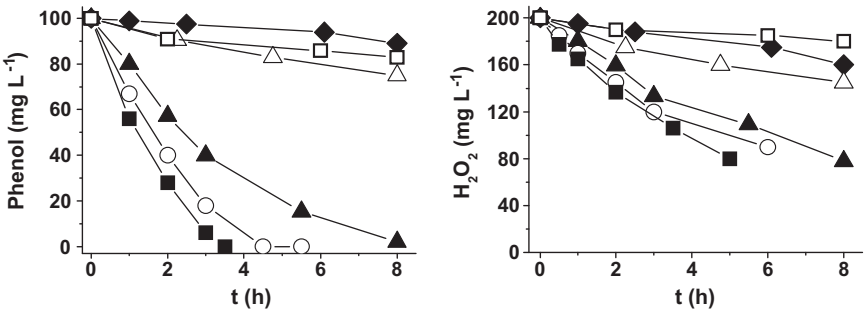

Fig. 10. Phenol disappearance (a) and H_2O_2 decomposition (b) using different gold supported D catalysts. Legend: (■) Au(0.1%)/FH_2, (○) Au(0.2%)/FH_2, (▲) Au(0.5%)/FH_2, (Δ) Au(0.5%)/FN_2, (♦) Au(0.5%)/F, (□) Au(0.1%)/FH_2 under dark conditions.

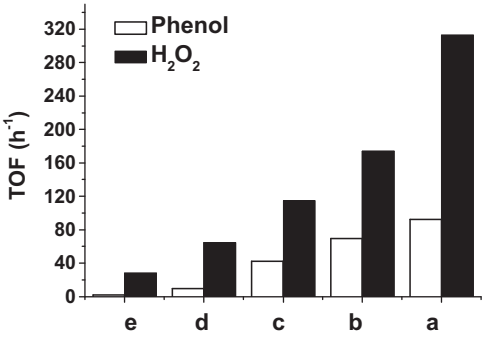

Fig. 11. TOF for phenol degradation and H_2O_2 decomposition using different gold supported D catalysts. Legend: (a) Au(0.1%)/FH_2, (b) Au(0.2%)/FH_2, (c) Au(0.5%)/FH_2, (d) Au(0.5%)/FN_2, (e) Au(0.5%)/F.

In order to further compare samples with different gold loading, the TOF values in which the number of molecules of substrate decomposed per gold atom and time unit is the catalytic parameter considered was determined (Fig. 11). Thus, the TOF values, both for phenol disappearance and H_2O_2 consumption, follow the expected general trend, increasing the activity of the catalyst when the particle size becomes smaller.

Additional experiments show that the heterogeneous Fenton reaction can also take place at quasi-neutral pH values although the catalytic activity decreases as the pH of the solution increases (Fig. S4). Importantly, the reaction can be performed using a low H_2O_2 to phenol molar ratio of 5.5 when the reaction was carried out at pH 4, but only 2.6 equiv. of H_2O_2 were consumed and there was a residual H_2O_2 concentration at final time of about 50%. This is remarkable since most of the heterogeneous Fenton reactions are carried out using a very large excess of H_2O_2 (up to 120,000 times) [18] and most of it is decomposed spuriously to O_2. Thus, our catalyst and conditions are highly favorable and unique in this type of processes. Also, the catalyst was reused for three times without significant lose of catalytic activity (Fig. S5). Gold leaching was also negligible (<1% of the initial Au in the photocatalyst in the first run) or not observed.

Finally, quenching experiments using DMSO as selective hydroxyl radical scavenger [14] indicate that phenol degradation takes place mainly through reaction with this highly oxidant species (Fig. S6).

4. Conclusions

Au NPs supported on treated-D NPs are excellent catalysts to cause the degradation of phenol by H_2O_2 through the generation of •OH radicals [13–15]. The interest of this catalyst compared to other solids is the high percentage of free •OH radicals that can be generated on the surface. However, the activity of this gold supported D NP material strongly depends on the gold average particle size and its distribution. In the present work we have shown that aerobic oxidation at moderate temperature of D surface besides decomposing the soot matter introduces oxygen functional groups. By annealing of these groups, particularly in the presence of H_2, D NPs suitable to be used as solid support for Au NPs can be obtained. This sample exhibits a notable catalytic activity and has an advantageous preparation method that does not require the use of liquid chemicals and does not generate liquid waste. In addition, the results obtained nicely match with the general conceptual framework that in order to achieve high catalytic activity in gold catalysis small Au NPs have to be obtained. We have found that even using in all cases the same preparation procedure based on polyol adsorption the average particle size remarkably depends on gold loading and the nature of the functional groups present on the diamond surface. Our study opens the way for novel preparation procedures in where the uses of large quantities of highly aggressive sulfuric acid or transition metals are avoided.

Acknowledgements

Financial support by the Spanish Ministry of Economy and Competitiveness (MINECO, Severo Ochoa program and CTQ 2012-32316) and Universidad Politécnica de Valencia (PAID-06-11, n° 2095) is gratefully acknowledged. We thank also to the EU funded TRAIN2 project for the partial funding of networking. SN thanks to the UPV for a lecturer contract.

Appendix A. Supplementary data

Supplementary data associated with this article can be found, in the online version, at http://dx.doi.org/10.1016/j.apcatb.2013.05.016.

References

[1] A. Abad, P. Concepción, A. Corma, H. García, Angewandte Chemie International Edition 44 (2005) 4066–4069.
[2] M. Haruta, M. Daté, Applied Catalysis A: General 222 (2001) 427–437.
[3] D. Astruc, F. Lu, J.R. Aranzaes, Angewandte Chemie International Edition 44 (2005) 7852–7872.
[4] A. Corma, P. Serna, Science 313 (2006) 332–334.
[5] M. Stratakis, H. Garcia, Chemical Reviews 112 (2012) 4469–4506.
[6] M.-C. Daniel, D. Astruc, Chemical Reviews 104 (2004) 293–346.
[7] A. Corma, H. Garcia, Chemical Society Reviews 37 (2008) 2096–2126.
[8] B.K. Min, C.M. Friend, Chemical Reviews 107 (2007) 2709–2724.
[9] M. Haruta, Catalysis Today 36 (1997) 153–166.
[10] T. Takei, T. Akita, I. Nakamura, T. Fujitani, M. Okumura, K. Okazaki, J. Huang, T. Ishida, M. Haruta, Adv. Catal. 55 (2012) 1–126.
[11] R. Martin, S. Navalon, M. Alvaro, H. Garcia, Applied Catalysis B: Environmental 103 (2010) 246–252.
[12] R. Martin, S. Navalon, J.J. Delgado, J.J. Calvino, M. Alvaro, H. Garcia, Chemistry A European Journal 17 (2011) 9494–9502.
[13] S. Navalon, R. Martin, M. Alvaro, H. Garcia, Angewandte Chemie International Edition 49 (2010) 8403–8407.

[14] S. Navalon, R. Martin, M. Alvaro, H. Garcia, ChemSusChem 4 (2011) 650–657.
[15] S. Navalon, M.d. Miguel, R. Martin, M. Alvaro, H. Garcia, Journal of the American Chemical Society 133 (2011) 2218–2226.
[16] J.J. Pignatello, E. Oliveros, A. Mackay, Critical Reviews in Environment Science and Technology 36 (2006) 1–84.
[17] S. Navalon, M. Alvaro, H. Garcia, Applied Catalysis B: Environmental 99 (2010) 1–26.
[18] A. Dhakshinamoorthy, S. Navalon, M. Alvaro, H. Garcia, ChemSusChem 5 (2012) 46–64.
[19] S. Navalon, A. Dhakshinamoorthy, M. Alvaro, H. Garcia, ChemSusChem 4 (2011) 1712–1730.
[20] K.J. Carroll, J.U. Reveles, M.D. Shultz, S.N. Khanna, E.E. Carpenter, Journal of Physical Chemistry C 115 (2011) 2656–2664.
[21] R.J. Joseyphus, K. Shinoda, D. Kodama, B. Jeyadevan, Materials Chemistry and Physics 123 (2010) 487–493.
[22] C. López-Santos, F. Yubero, J. Cotrino, A.R. González-Elipe, Diamond and Related Materials 20 (2011) 49–56.
[23] A. Abad, A. Corma, H. García, Chemistry A European Journal 14 (2008) 212–222.
[24] S. Osswald, G. Yushin, V. Mochalin, S.O. Kucheyev, Y. Gogotsi, Journal of the American Chemical Society 128 (2006) 11635–11642.
[25] J.L. Figueiredo, F.R. Pereira, M.M.A. Freitas, J.J.M. Órfao, Carbon 37 (1999) 1379–1389.
[26] J.-H. Zhou, Z.-J. Sui, J. Zhu, P. Li, D. Chen, Y.-C. Dai, W.-K. Yuan, Carbon 45 (2007) 785–796.
[27] H.A. Girard, J.C. Arnault, S. Perruchas, S. Saada, T. Gacoin, J.-P. Boilot, P. Bergonzo, Diamond and Related Materials 19 (2010) 1117–1123.
[28] S. Zeppilli, J.C. Arnault, C. Gesset, P. Bergonzo, R. Polini, Diamond and Related Materials 19 (2010) 846–853.
[29] A. Dhakshinamoorthy, S. Navalon, D. Sempere, M. Alvaro, H. Garcia, ChemCatchem 5 (2013) 241–246.
[30] Z. Wang, Q. Zhang, D. Kuehner, A. Ivaska, L. Niu, Green Chemistry 10 (2008) 907–909.